

NASA TM X- 55738

3 AN EVALUATION OF AN
OPERATIONAL SOUNDING ROCKET
TO FULFILL A NEW
100 KILOMETER REQUIREMENT 6

N 67-22075

FACILITY FORM 602	(ACCESSION NUMBER)	(THRU)
	10 / 9RS 22-21A	1
	(PAGES)	(CODE)
	TMX-55738-29E	31
	(NASA CR OR TMX OR AD NUMBER)	(CATEGORY)

9 MARCH 1967 10



— GODDARD SPACE FLIGHT CENTER —
GREENBELT, MARYLAND 3

1136

X-721-67-144

AN EVALUATION OF AN OPERATIONAL
SOUNDING ROCKET TO FULFILL
A NEW 100 KILOMETER REQUIREMENT

6 Mark B. Nolan
Edward E. Mayo
Spacecraft Integration and
Sounding Rocket Division

March 1967

Goddard Space Flight Center
Greenbelt, Maryland

CONTENTS

	<u>Page</u>
Abstract	1
Introduction	1
Payload - Apogee Performance.	2
Static Stability	4
Weight and Balance	4
Static Margin and Natural Pitch Frequency	6
Flight Dynamics.	7
Vehicle Parameters	8
Undisturbed Roll Rate and Pitch Frequency.	9
Steady - State Solution.	9
Dynamic Solution	11
Space Coning Motion	12
Fin Cant Selection	12
Conclusions	13
List of Symbols	13
References	14

ILLUSTRATIONS

<u>Figure</u>		<u>Page</u>
1	Nike Tomahawk Sounding Rocket	2
2	Tomahawk Payload-Apogee Performance	4
3	Tomahawk Nose Configuration Selection	4
4	Tomahawk Drag (3:1 Ogive Nose)	4
5	Total Vehicle Length (Constant Density Payload)	5
6	Tail Normal Force Coefficient	6
7	Static Stability Axis System	6
8	Tomahawk Minimum Static Margin	8
9	Tomahawk Natural Pitch Frequency (3:1 Ogive Nose)	8
10	Orientation of Tomahawk Asymmetries	8
11	Undisturbed Roll Rates	9
12	Tomahawk Non-Rolling Trim	10
13	Magnification Factor	10
14	Tomahawk Rolling Trim	10
15	Required Center-of-Gravity Offset to Maintain Lock-in	11
16	Dynamic Roll Rates	11
17	Dynamic Rolling Trim	12
18	Comparison of the Steady State and Dynamic Solutions	12
19	Effect of Aerodynamic Pitch Damping on the Rolling Trim	12
20	Space Coning Motion	12

TABLES

<u>Tables</u>	<u>Page</u>
1 "D" Region Experiment Vehicle Requirements	1
2 Tomahawk Weight-Time History (Less Gross Payload Weight)	2
3 Tomahawk Sea Level Thrust-Time History	2
4 Tomahawk Coasting Drag Coefficient (C_{D_C}) for Various Nose Configurations	3
5 Tomahawk Performance Variation	4
6 Tomahawk Weight and Balance Data	5
7 Tomahawk Payload Geometry	5
8 Tomahawk Normal Force Coefficient	6
9 Tomahawk Center of Pressure Location	7

AN EVALUATION OF AN OPERATIONAL SOUNDING ROCKET
TO FULFILL A NEW 100 KILOMETER REQUIREMENT

Mark B. Nolan
Edward E. Mayo
Goddard Space Flight Center
Greenbelt, Maryland

Abstract

The payload-apogee altitude performance, static stability, and dynamic motions of the Tomahawk vehicle (second stage of the Nike-Tomahawk system) are analyzed with respect to its ability to meet a new requirement for a 100-kilometer sounding rocket. The vehicle has the impulse to lift the required payload to the required altitude and the payload can be increased by replacing the standard nose cone (3:1 ogive) with a lower drag configuration. The single-stage vehicle is very drag-sensitive, losing 4000 feet in apogee for each 1-percent increase in drag. The fins produce adequate stability to fly payloads as light as 65 pounds for the 3:1 ogive nose. The optimum fin cant from a flight dynamics standpoint was determined to be 35 minutes, with a resulting peak roll rate of 10 cps. If required by the experiment, the peak roll rate can be reduced to 6.5 cps while the resulting rolling trim remains less than 5 degrees. The vehicle asymmetries evaluated were the maximum manufacturing tolerances and were oriented to give maximum degradation to roll rate at resonance.

Introduction

In the continuing investigation of the upper atmosphere, the scientific community has become increasingly interested in a layer of the earth's atmosphere known as the "D" region. The "D" region is the lowest layer in the ionosphere, extending from approximately 70 to 120 kilometers. It is through this region that the exchange between the ionized upper atmosphere and the nonionized lower atmosphere occurs.

For a class of experiments to be conducted in this region NASA has established a requirement for a vehicle with the performance characteristics given in Table 1. A partially successful flight of a Tomahawk vehicle (second stage of the Nike Tomahawk system)⁽¹⁾ indicated a performance comparable with the vehicle requirements of Table 1. The Tomahawk vehicle, if acceptable as a single-stage rocket, has the obvious advantage of being a fully operational system in the two-stage version.

This paper outlines the procedures applied by the Goddard Space Flight Center in the evaluation of a vehicle with respect to a new requirement, and presents the results in the specific case of the Tomahawk vehicle. In the initial phase of the evaluation, the vehicle payload-apogee altitude performance is determined by varying the launch angle, gross payload weight, and nose-cone (drag) configuration. Then, if altitude performance is satisfactory, static stability is evaluated for the range of variables analyzed in the initial phase. A third phase evaluates the dynamic motions of the vehicle and assesses its sensitivity to roll lock-in. An analysis of the aerodynamic heating and the structural integrity of the system is also necessary. However, for the Tomahawk, this is now being done under contract and will therefore not be presented in this paper.

Payload weight*	50 pounds
Apogee altitude	50 to 120 kilometers
Velocity restrictions**	$M_{\infty} \leq 3.00$ @ 60 kilometers $M_{\infty} \leq 1.50$ @ 100 kilometers
Vehicle dynamic motion restrictions	Space coning half angle $\leq 10^{\circ}$ Maximum roll rate ≤ 10 cps

* A conservative estimate of the gross payload weight is 80 pounds for a Tomahawk vehicle with a net payload weight of 50 pounds.

** This velocity restriction limits the apogee altitude to approximately 106 kilometers (350,000 feet).

TABLE 1 "D" REGION EXPERIMENT VEHICLE REQUIREMENTS

Payload-Apogee Performance

The payload-apogee performance of the single-stage Tomahawk (Figure 1) was determined for gross payload weights of 40 to 100 pounds and launch angles of 75 to 90 degrees for the three nose configurations under consideration, a 3:1 ogive, a 5:1 ogive, and a 5:1 cone. Performance trajectories were calculated by a particle trajectory digital computer program assuming Wallops Island as the launch site.

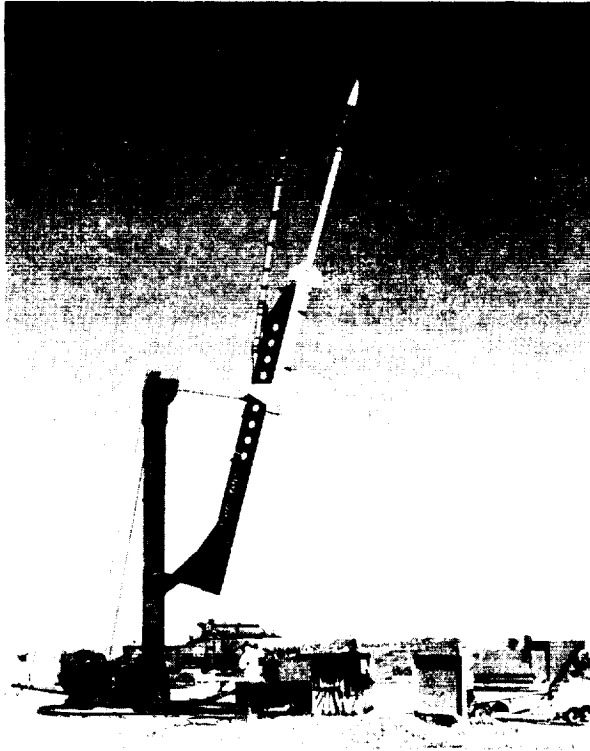


FIGURE 1. NIKE TOMAHAWK SOUNDING ROCKET

The required input data for the program are weight, drag, and thrust-time history, where the drag is at zero angle-of-attack^(2,3). The Tomahawk weight-time history and sea level thrust-time history are given in Tables 2 and 3, respectively. Since the Tomahawk, as the second stage of the Nike-Tomahawk system, flies at supersonic velocities, there was no subsonic drag and the transonic drag was obtained by extrapolating the data to Mach one. The author's calculations⁽⁴⁻⁸⁾ verified the transonic drag level and have extended the estimated drag to subsonic Mach numbers. The results of the analysis that follows show that the vehicle performance is insensitive to the subsonic drag level. A 50 percent reduction in subsonic drag results in only a 300-foot increase in altitude for a 350,000-foot apogee. It will be shown later that, while insensitive to subsonic drag, the vehicle is very sensitive to supersonic drag.

TIME (sec)	WEIGHT (lb)
0	340.00
0.25	329.64
0.50	317.29
4.00	341.82
5.00	292.79
6.00	248.05
7.00	207.99
8.00	171.62
8.50	155.307
8.70	150.00
9.00	143.83
9.50	143.00
999.00	143.00

TABLE 2. TOMAHAWK WEIGHT-TIME HISTORY
(LESS GROSS PAYLOAD WEIGHT)

TIME (sec)	THRUST (lb)
0	0
0.10	13847
0.17	12665
0.22	12766
0.34	11736
0.90	12030
1.10	12080
1.60	11785
2.20	11588
3.00	11736
3.50	11686
5.00	11293
5.30	10999
6.00	9968
7.00	8888
7.81	8347
8.00	8004
8.15	8053
8.50	7268
8.72	5892
9.20	442
9.50	0

TABLE 3. TOMAHAWK SEA LEVEL
THRUST-TIME HISTORY
(NOZZLE EXIT AREA = 0.4035 SQUARE FOOT)

Data from the above references were also used to modify the drag curve of the 3:1 ogive configuration to apply to the 5:1 ogive and cone configurations. This was accomplished by subtracting the pressure drag of a 3:1 ogive nose from the basic drag data* and then adding the pressure drag for the 5:1 ogive and cone configurations. The resulting values are presented in Table 4 for both coasting and thrusting conditions.

* Letter of Sandia Corporation to John Lane, dated January 21, 1965. Subject: Performance and Aerodynamic Data for the Nike Tomahawk Rocket System

These data were used in computing vehicle performance for the range of parameters mentioned earlier. A summary plot of the apogee as a function of gross payload weight and launch angle is

given in Figure 2 and the results of a study of the vehicle sensitivity to variations in the input parameters are given in Table 5.

3:1 OGIVE CONFIGURATION		5:1 OGIVE CONFIGURATION		5:1 CONE CONFIGURATION	
MACH NO.	C_{DC}	MACH NO.	C_{DC}	MACH NO.	C_{DC}
0.00	0.640	0.0	0.610	0.0	0.625
0.25	0.645	0.25	0.612	0.25	0.625
0.50	0.650	0.50	0.621	0.50	0.630
0.60	0.660	0.60	0.630	0.60	0.650
0.70	0.700	0.70	0.650	0.70	0.670
0.80	0.810	0.80	0.710	0.80	0.730
0.90	0.978	0.90	0.860	0.90	0.910
1.00	1.142	1.00	1.055	1.00	1.1000
1.10	1.205	1.10	1.125	1.10	1.1600
1.20	1.190	1.25	1.0951	1.25	1.1095
1.30	1.110	1.60	0.9350	1.60	0.9417
1.60	1.00	1.90	0.8385	1.90	0.8412
1.90	0.900	2.20	0.7409	2.20	0.7416
2.20	0.800	2.50	0.6730	2.50	0.6725
2.50	0.730	2.90	0.5954	2.90	0.5936
2.90	0.650	3.25	0.5475	3.25	0.5450
3.25	0.600	3.50	0.5140	3.50	0.5110
3.50	0.565	3.75	0.4803	3.75	0.4869
3.75	0.540	4.00	0.4712	4.00	0.4683
4.00	0.520	4.30	0.4522	4.30	0.4480
4.30	0.500	4.75	0.4254	4.75	0.4208
4.75	0.472	5.25	0.3991	5.25	0.3943
5.25	0.445	6.00	0.3700	6.00	0.3648
6.00	0.415	7.00	0.3359	7.00	0.3307
7.00	0.380	9.00	0.2725	9.00	0.2675
9.00	0.315	999.00	0.2725	999.00	0.2675
999.00	0.315				

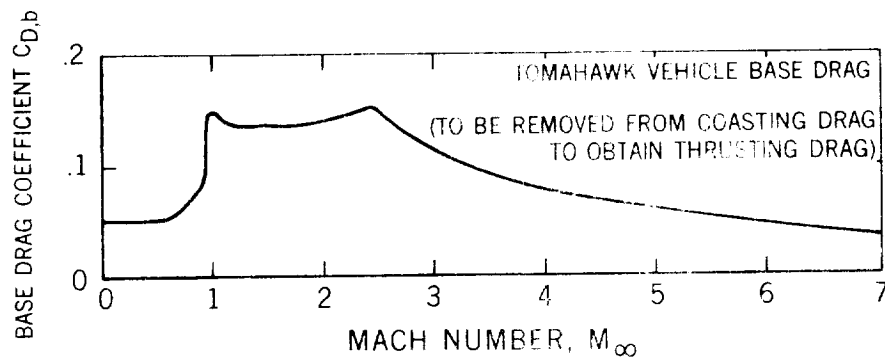


TABLE 4 TOMAHAWK COASTING DRAG COEFFICIENT (C_{DC}) FOR VARIOUS NOSE CONFIGURATIONS *

* Aerodynamic reference area = 0.4418 ft.²

Nine inch payload in all cases.

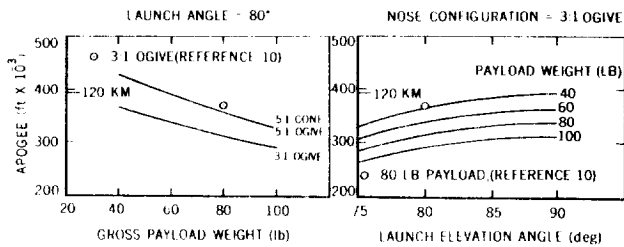


FIGURE 2. TOMAHAWK PAYLOAD-APOGEE PERFORMANCE

PARAMETER	MAGNITUDE OF VARIATION	APOGEE ALTITUDE CHANGE (ft)
DRAG	+1%	- 4,000
IMPULSE	+1%	+11,000
WEIGHT	+1 pound	- 1,800

TABLE 5 TOMAHAWK PERFORMANCE VARIATION*

* Reference 10

Next, it was necessary to find the Tomahawk configuration that fulfilled the vehicle requirement of lifting 80 pounds to a maximum altitude without exceeding velocity restrictions. In Figure 3, the Mach number at 60 and 100 kilometers is plotted for the 3:1 ogive and 5:1 cone configurations as a function of payload weight. A typical launch angle for the Wallops Island complex, 80 degrees, was assumed. For this angle, the maximum altitude attainable, within velocity restrictions, is 345,000 feet. Maximum payload is 55 pounds for the 3:1 ogive and 90 pounds for the 5:1 cone (Figure 3). To lift the 80-pound payload it is necessary to use the 5:1 cone configuration and ballast the vehicle to insure a gross payload weight of 90 pounds. The 5:1 cone was chosen over the 3:1 ogive because of the increased stability of the cone configuration,⁽⁹⁾ the altitude performance of the two nose configurations being almost identical.

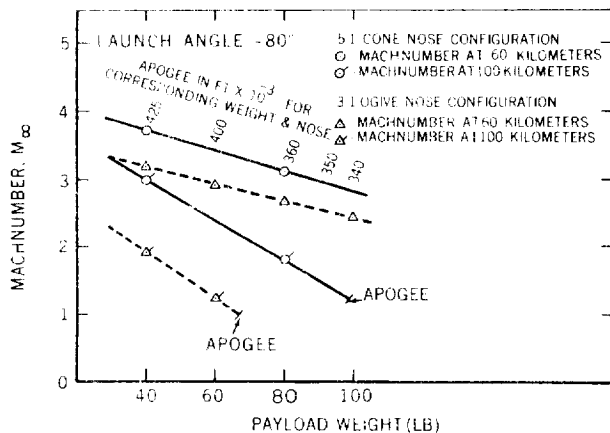


FIGURE 3. TOMAHAWK NOSE CONFIGURATION SELECTION

Figure 4 presents an analytically computed drag curve for the 3:1 ogive configuration supplied by the manufacturer⁽¹⁰⁾ along with the drag curve used in the performance study. Estimated performance on the basis of the reduced drag computed by the manufacturer would permit use of the 3:1 ogive configuration to lift 80 pounds to a maximum altitude of approximately 110 kilometers. The actual performance will fall between the two drag cases and the actual drag will be verified by flight test. From the above calculations, and data, it is concluded that the Tomahawk vehicle meets the specified performance requirements.

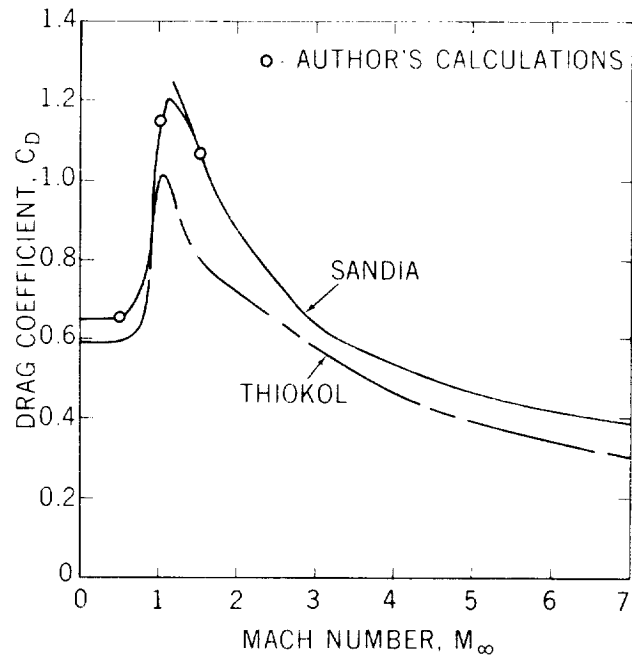


FIGURE 4. TOMAHAWK DRAG (3:1 OGIVE NOSE)

Static Stability

Static vehicle stability was calculated for the range of payload weights and nose configurations evaluated in the preceding section. The present analysis will be limited to a single launch angle (80 degrees).

Weight and Balance

Vehicle weight, center of gravity, and pitch and roll moments of inertia were calculated by a computer program* developed by the GSFC Flight Performance Section. The program combines the motor and payload weight and balance to arrive at the total vehicle weight and balance as a function of time in flight.

* Memo from E. E. Mayo to E. F. Sorgnit, dated 3 June 1964; Subject: Weight, Center of Gravity, Pitch and Roll Moment of Inertia Determination Program.

The Tomahawk motor (TE416) weight and balance data * for conditions prior to launch and after burnout are presented in Table 6. Payload center of gravity, and pitch and roll moments of inertia were computed from the payload weight and geometry data. Payload length was calculated assuming a constant density payload, specific gravity equal to 0.80⁽¹¹⁾, and total volume utilization. The required cylindrical extension for each of the nose configurations and payload weights is presented in Table 7. Figure 5 gives the resultant total vehicle lengths versus gross payload. Total vehicle weight, center of gravity location (in feet from the base), and pitch moment of inertia were computed for the above configurations and are used to compute the static margin and natural pitch frequency in the following section.

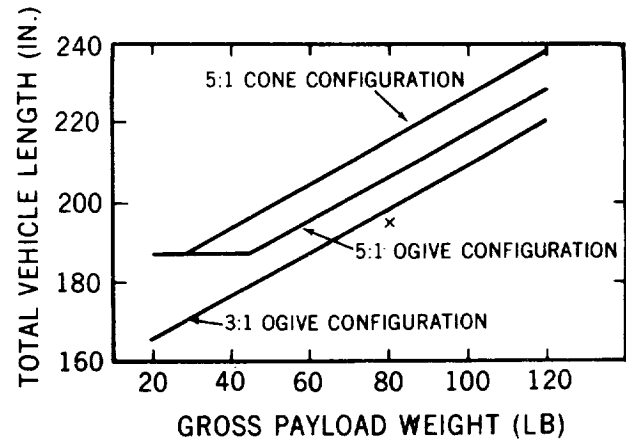


FIGURE 5. TOTAL VEHICLE LENGTH (CONSTANT DENSITY PAYLOAD)

Center of gravity location of empty motor plus fins	3.458 ft
Center of gravity location of loaded motor plus fins	5.875 ft
Center of gravity location of propellant lost	6.746 ft
Distance from base to payload adapter	11.87 ft
Weight of motor empty plus fins	143 lb
Weight of motor loaded plus fins	540 lb
Pitch moment of inertia of motor empty plus fins	63.2 slug-ft ²
Pitch moment of inertia of motor loaded plus fins	207 slug-ft ²

TABLE 6. TOMAHAWK WEIGHT AND BALANCE DATA

CONFIGURATION	PAYLOAD WEIGHT (lb)	NOSE LENGTH (ft)	CYLINDRICAL LENGTH (ft)	TOTAL PAYLOAD LENGTH (ft)	TOTAL VEHICLE LENGTH (ft)	TOTAL VEHICLE LENGTH (in)
3:1 Ogive	40	2.25	.58	2.83	14.683	176.19
	60	2.25	1.50	3.75	15.596	187.16
	80	2.25	2.41	4.66	16.513	198.16
	100	2.25	3.38	5.63	17.471	209.66
5:1 Ogive	40	3.75	0	3.75	15.596	187.16
	80	3.75	1.61	5.36	17.209	206.51
5:1 Cone	40	3.75	.56	4.31	16.159	193.91
	80	3.75	2.38	6.13	17.980	215.76
	110	3.75	3.75	7.50	19.380	232.16

TABLE 7. TOMAHAWK PAYLOAD GEOMETRY

* Letter of Sandia Corporation to John Lane, dated January 21, 1965

Static Margin and Natural Pitch Frequency

Static margin, static stability parameter, and natural pitch frequency of the Tomahawk vehicle have been calculated by a computer program developed in-house*. The center of gravity location and pitch moment of inertia calculated above are required inputs in addition to vehicle normal force coefficient, ($C_{N\alpha}$), center of pressure location ($X_{c.p.}$) and the velocity and altitude-time histories of the vehicle trajectories.

The $C_{N\alpha}$ and $X_{c.p.}$ of the Tomahawk vehicle** for the 3:1 ogive nose and 209 inch overall length were modified⁽⁸⁾ for the 5:1 ogive and cone configurations. Experimental data^(8, 12) on configurations with varying afterbody lengths indicate that there is little or no increase in $C_{N\alpha}$ or $X_{c.p.}$ for afterbody length in excess of 10 diameters. Since all Tomahawk vehicles evaluated had afterbody lengths in excess of 10 diameters, the $C_{N\alpha}$ of the total vehicle and $X_{c.p.}$ of the nose and afterbody (minus fins) were considered a function of the nose configuration and Mach number only. The $C_{N\alpha}$ of the total vehicle is given by

$$C_{N\alpha}(T) = C_{N\alpha}(N+A) + C_{N\alpha}(F+I)$$

NORMAL FORCE COEFFICIENT $C_{N\alpha}$			
Mach No.	3:1 Ogive	5:1 Ogive	5:1 Cone
1.20	30.997	30.997	30.997
1.30	29.749	29.794	29.794
1.50	26.528	26.528	26.528
1.65	23.606	23.606	23.606
2.00	19.481	19.481	19.481
2.25	17.762	17.590	17.475
2.50	16.215	16.043	15.928
3.00	14.037	13.808	13.784
3.50	12.605	12.548	12.490
4.00	11.516	11.459	11.402
4.50	10.714	10.600	10.599
5.00	10.199	10.141	10.084
5.50	9.798	9.969	9.855
6.00	9.511	9.855	9.740
6.50	9.282	9.798	9.626
7.00	9.110	9.740	9.626

TABLE 8. TOMAHAWK NORMAL FORCE COEFFICIENT

and is tabulated in Table 8 as a function of Mach number for the three nose configurations. The fin plus interference normal force coefficient, $C_{N\alpha}(F+I)$, was computed by subtracting the 3:1 ogive nose normal force⁽⁸⁾ from the total $C_{N\alpha}$ of the vehicle**:

$$C_{N\alpha}(F+I) = C_{N\alpha}(T) (3:1 \text{ ogive})^{**} - C_{N\alpha}(N+A) (3:1 \text{ ogive}) (\text{Ref. 8}).$$

It is also computed by analytical methods. The fin plus interference normal force coefficient obtained by both means, is plotted versus Mach number in Figure 6. While neither curve can be used to verify the other, the fact that they are both in agreement indicates that the $C_{N\alpha}$ data are valid. Although the $X_{c.p.}$ of the nose and afterbody (minus fins) is independent of the afterbody length for the Tomahawk configurations, the total vehicle $X_{c.p.}$ measured from the base is a function of the vehicle length. This is demonstrated by the equation

$$X_{c.p.} = \frac{C_{N\alpha}(N+A) (L - X_{c.p.}) + C_{N\alpha}(F+I) (C)}{C_{N\alpha}(T)}$$

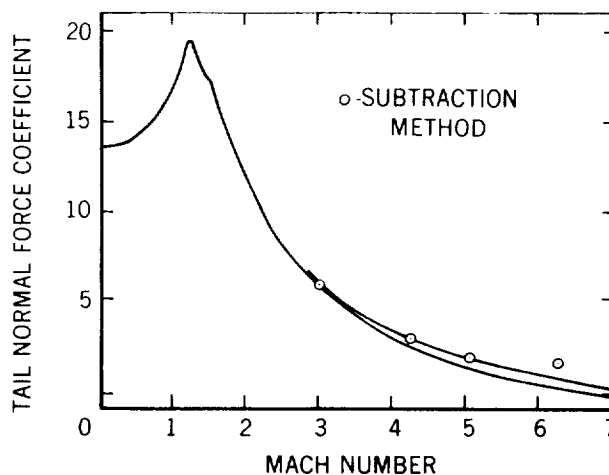


FIGURE 6. TAIL NORMAL FORCE COEFFICIENT

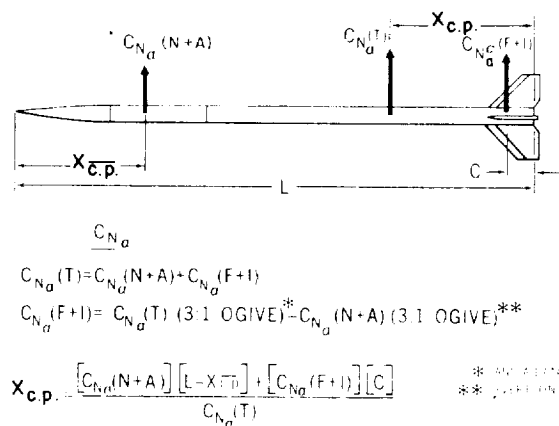


FIGURE 7. STATIC STABILITY AXIS SYSTEM

The axis system for the above calculations is presented in Figure 7. The $X_{c.p.}$ tabulated as a function of Mach number, nose configurations, and vehicle length is presented in Table 9.

*Memo, 9 July 1964, E. E. Mayo to Flight Performance Section Files, Subject: Static Stability and Natural Frequency Program.

**Letter, 21 Jan., 1965, to John Lane from the Sandia Corp., Subject: Performance and Aerodynamic Data for the Tomahawk Rocket System.

CONFIGURATION	CENTER OF PRESSURE LOCATION					
	MACH NUMBER	40 LB PAYLOAD	60 LB PAYLOAD	80 LB PAYLOAD	100 LB PAYLOAD	110 LB PAYLOAD
3:1 Ogive	1.20	1.80	1.85	1.88	1.90	
	1.50	1.94	2.00	2.15	2.17	
	1.75	2.15	2.25	2.46	2.50	
	2.00	2.46	2.61	2.81	2.85	
	2.50	3.09	3.30	3.55	3.60	
	3.00	3.59	3.82	4.04	4.17	
	3.50	3.97	4.20	4.41	4.64	
	4.00	4.30	4.53	4.80	5.05	
	5.00	4.86	5.11	5.41	5.70	
	6.00	5.36	5.62	5.92	6.23	
	7.00	5.76	6.10	6.35	6.67	
	8.00	6.15	6.52	6.75	7.06	
5:1 Ogive	1.20	1.82		1.84		
	1.50	2.00		2.00		
	1.75	2.24		2.35		
	2.00	2.55		2.72		
	2.50	3.13		3.40		
	3.00	3.57		3.93		
	3.50	3.95		4.37		
	4.00	4.31		4.73		
	5.00	4.95		5.38		
	6.00	5.51		5.90		
	7.00	6.02		6.36		
	8.00	6.50		6.75		
5:1 Cone	1.20	1.78		1.81		1.90
	1.50	1.88		2.00		2.17
	1.75	2.05		2.25		2.50
	2.00	2.28		2.59		2.90
	2.50	2.90		3.30		3.65
	3.00	3.45		3.85		4.20
	3.50	3.88		4.30		4.65
	4.00	4.27		4.67		5.07
	5.00	4.95		5.34		5.80
	6.00	5.51		5.85		6.40
	7.00	6.00		6.30		6.93
	8.00	6.45		6.68		7.35

TABLE 9. TOMAHAWK CENTER OF PRESSURE LOCATION
(MEASURED IN FEET FROM NOZZLE EXIT PLANE)

A summary plot of the minimum static margin for the configurations investigated is given in Figure 8. An increase in payload density, whether resulting from adding weight to the current configuration or reducing the size of the current configuration, will increase stability above that indicated in Figure 8. A decrease in payload density will decrease stability and the individual configuration will have to be evaluated individually. Current wind tunnel tests of the Tomahawk configuration indicate that the $X_{c.p.}$ as used in this study was conservative. Preliminary results of the test indicated a minimum static margin approximately 1.0 caliber more stable. With the increased stability, the Tomahawk configuration can be flown with payloads as light as 65 pounds for the 3:1 ogive configuration and meet the criteria of a minimum static margin of at least 2.0 calibers. The natural pitch frequency for the 3:1 ogive configuration, is plotted versus time in flight in Figure 9 and is calculated as

$$\omega = \sqrt{\frac{-C_m \alpha \bar{q} S d}{I}}$$

The above data are the input to the next phase of the analysis, in which the dynamic response of the vehicle to the flight environment is evaluated.

Flight Dynamics

The dynamic motions of the single-stage Tomahawk vehicle were computed by the Lockheed RPM computer program^(13, 14), which calculates the angular motions of the vehicle about a predetermined particle trajectory. This small-angle analysis approach is particularly applicable to the single-stage Tomahawk,

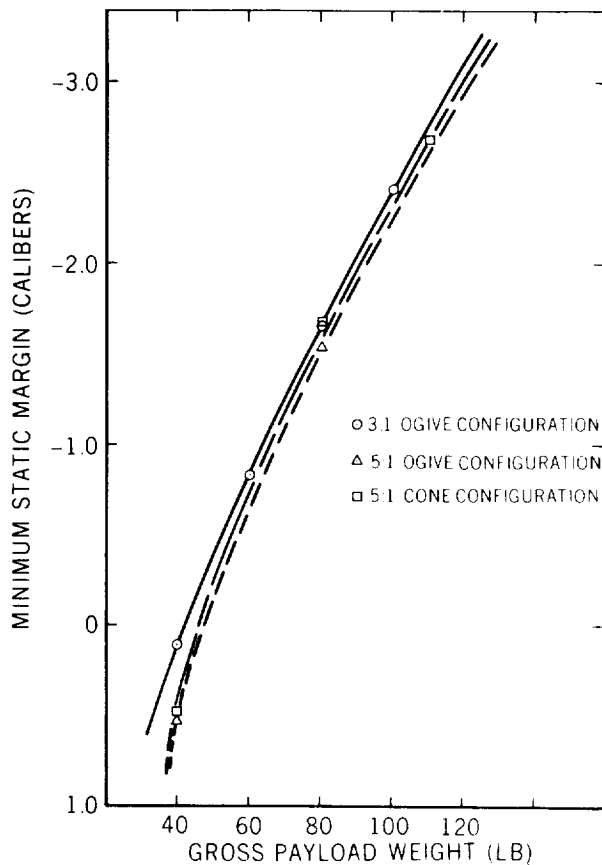


FIGURE 8. TOMAHAWK MINIMUM STATIC MARGIN

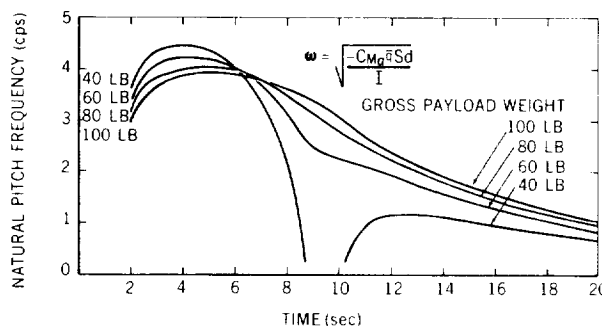


FIGURE 9. TOMAHAWK NATURAL PITCH FREQUENCY (3:1 OGIVE NOSE)

since the vehicle must fly at relatively small angles of attack to survive the aerodynamic environment ($\bar{q} \rightarrow 20,000$ feet).

The program has two computation options. The first is the steady-state solution, which assumes that the vehicle is in pitch-roll resonance throughout the trajectory. The nonrolling trim, magnification factor, and resultant total angle of attack (also referred to as the rolling trim) are computed as a function of time in flight. The steady-state solution also computes the center of gravity offset required to maintain pitch-roll resonance for a specific aerodynamic and thrust misalignment and fin cant angle. The second option is the dynamic solution, which computes the vehicle response

to a specific aerodynamic and thrust misalignment and center of gravity offset for a given fin cant.

Vehicle Parameters

The trajectory used in this analysis was a nominal sea-level launch, 80-degree quadrant-angle, particle trajectory presented in the most recent flight test proposal (10). The orientation of Tomahawk thrust and aerodynamic misalignments to be evaluated here (2, 15) is diagrammed in Figure 10. Fin misalignment is not utilized in the RPM program computations in degrees as given in the figure, but rather, as aerodynamic misalignment moment coefficient, C_{m0} . The program input format requires a constant value of C_{m0} , whereas the value of C_{m0} for a constant fin misalignment of 0.20 degree varies from 0.25 to 0.20 as a function of time in flight. Since the rolling trim, which results in part from C_{m0} , is insignificant throughout the trajectory except in the vicinity of resonance, the value of C_{m0} corresponding to the time of resonance was used in this study.

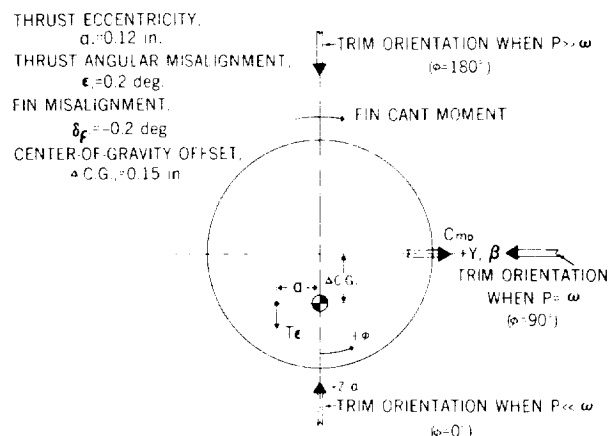


FIGURE 10. ORIENTATION OF TOMAHAWK ASYMMETRIES

A maximum center-of-gravity offset ($\Delta C.G.$) of 0.15 inch has been assumed for this analysis. An evaluation of the maximum possible vehicle $\Delta C.G.$ for the Tomahawk is not available; however, a study has been performed on a similar vehicle the Apache. The maximum $\Delta C.G.$ was determined to be 0.066 inch.* This value was rounded off to 0.10 inch and scaled to the Tomahawk vehicle by a ratio of the respective body diameters. The center-of-gravity offset calculated in this manner is considered conservative. It can be seen from the results of this study that a center-of-gravity offset of twice the value will be acceptable for the recommended fin cant setting.

The misalignment and offsets cited above are of random orientation. For this analysis, the misalignments and offsets are aligned in a worst-case condition; that is, oriented to give the maximum degradation to roll at resonance (Figure 10).

*Memo, 10 April 1964, D. J. Hershfeld to R. C. Baumann. Subject: Principal Tilt Axis (PAT) of Apache and Payload.

Undisturbed Roll Rate and Pitch Frequency

The Tomahawk vehicle has four wedge-slab fins, as shown in Figure 1, which are canted to produce the vehicle roll. The steady-state roll rate of canted fins is a function of the velocity and cant angle:

$$p_{ss} = A_1 V \delta$$

The constant A_1 is a function of the fin geometry as determined from strip theory. From this equation, it can be seen that, for a linear velocity time-history (such as the nominal trajectory), the roll rate increases linearly from ignition to burnout. The slope of the curve depends on the fin-cant angle. The roll rate-time histories for the range of fin cants were computed by the RPM program assuming no misalignments or offsets. The undisturbed roll rates and undamped natural pitch frequency versus time from launch are presented in Figure 11, as well as peak roll rate, as a function of fin cant angle. The fin-cant angles to be investigated in this study are now limited to a range of 0 to 35 minutes of a degree due to the vehicle requirements listed in Table 1, limiting the roll rate to 10 cps. The space or vacuum roll rate was 65.5 percent of the peak roll rate for all fin cants investigated.

Steady-State Solution

The static (or nonrolling) trim angle of attack is a result of the aerodynamic and thrust misalignments,

$$\alpha_{st} = \frac{R_o C_{m_2}}{-C_{m\alpha}} + \frac{r_c T \epsilon}{(-C_{m\alpha}) \bar{q} S d}$$

The nonrolling trim for both aerodynamic misalignments (C_{m_2} 0.25 and 0.26) is given in Figure 12. The step decrease in the static trim is due to thrust termination, while the variation before and after burnout is due to the variation in Mach number and dynamic pressure. For the spinning sounding rocket, the static trim is magnified as the vehicle traverses pitch-roll resonance. In the undamped case, the angle of attack diverges to infinity. However, with damping in the system, the static trim is magnified by a finite value which for the Tomahawk is presented in Figure 13. Magnification factor = U/b ,

$$b = \frac{R_o \bar{q} a}{m v \omega} \left[C_{L\alpha} (1-\nu) + \frac{m d^2}{I} \left(C_{mq} + C_{n_p \alpha} \right) \right]$$

$$U = \frac{R_o T}{m v \omega (1-\nu)} + \frac{R_o T r_c \epsilon}{I \bar{q} I_{sp} \omega}$$

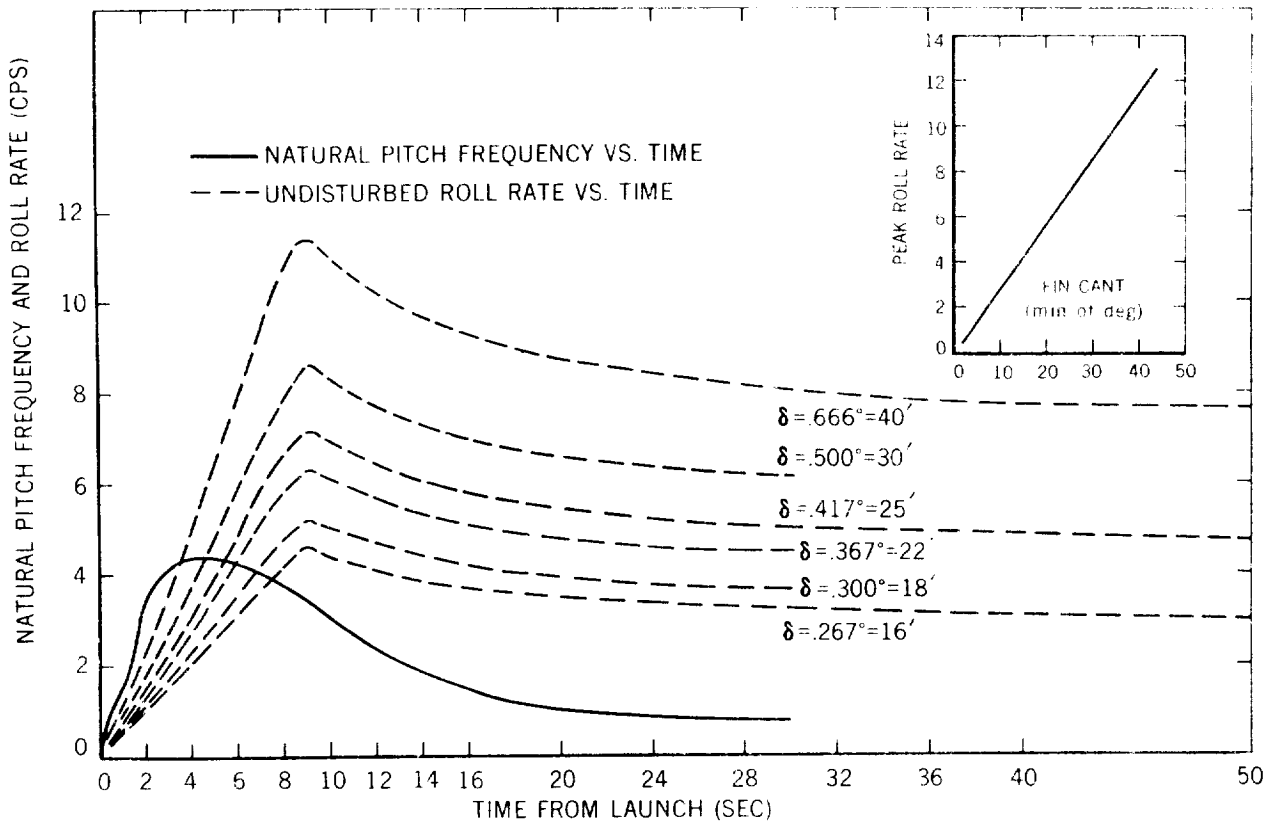


FIGURE 11. UNDISTURBED ROLL RATES

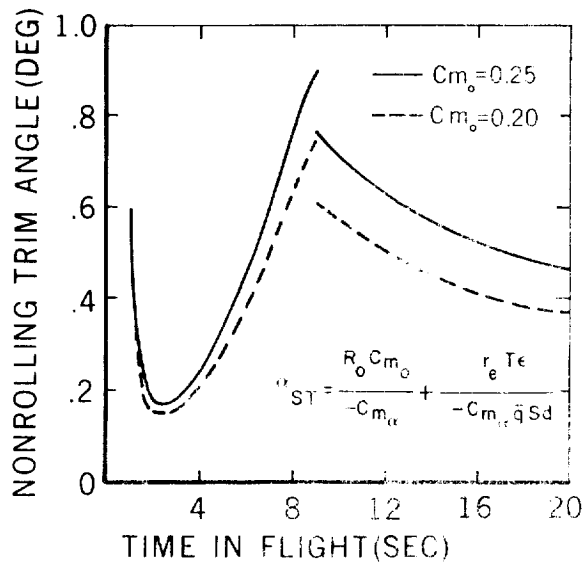


FIGURE 12. TOMAHAWK NON-ROLLING TRIM

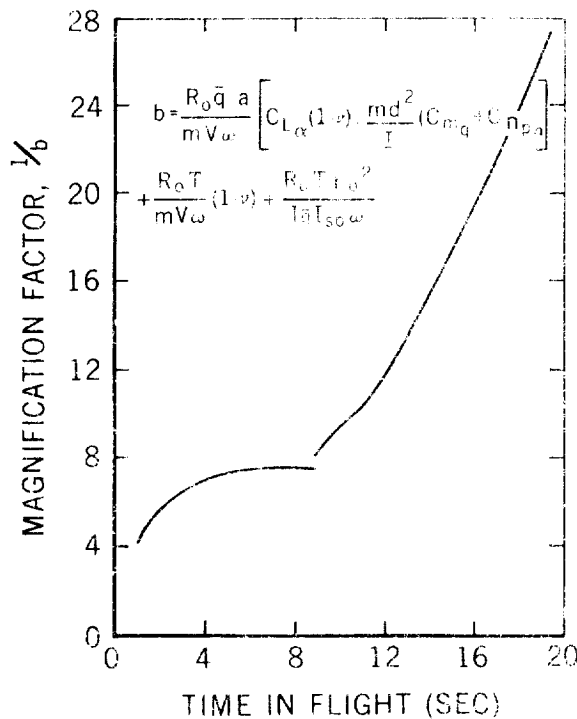


FIGURE 13. MAGNIFICATION FACTOR

The step increase in the magnification at burn-out is due to that decrease in the damping, resulting from thrust termination. The magnification factor increases with time in flight due to decreasing density.

The steady-state solution ($\rho = \omega$) of the RPM program was utilized to compute the total or rolling-trim angle of attack for the two values of C_{m_0} :

$$\alpha_T = \frac{\alpha_{st}}{b}$$

The resultant rolling trim is presented in Figure 14. This figure shows that resonance should occur as early as possible in order to limit the rolling-trim amplitude. It is particularly undesirable to have resonance after thrust termination where the total angle-of-attack approaches infinity.

The steady-state solution was also used to compute the center-of-gravity offset required to maintain lock-in as a function of time in flight:

$$\Delta C.G. = \frac{12d}{\alpha_t C_{N_\alpha}} \left[c C_{l_\beta} - C_{l_p} \left(\frac{\omega d}{2V} \right) - \frac{T_e a}{12 \bar{q} S d} \right]$$

For sounding rockets with canted fins, this is a logical approach since the vehicle must pass through resonance. The foregoing $\Delta C.G.$ calculation can be used to determine the time at which the vehicle will break out of pitch-roll resonance, as in Figure 15. Once the vehicle breaks out of roll lock-in, the roll rate will return to the undisturbed value, and the foregoing calculation is no longer valid.

The steady-state magnitude of the total angle-of-attack at resonance can be determined from the data now available. For example, assume the lift cant is 22 minutes and a center-of gravity offset is 0.15 inch. The vehicle enters into resonance at 5.57 seconds where the $\Delta C.G.$ curve crosses zero (Figure 15) and breaks out of resonance at 6.41 seconds when the $\Delta C.G.$ curve exceeds the 0.15 inch offset. As seen in Figure 14, the total angle-of-attack will be 3.51 degrees when the vehicle breaks out at 6.41 seconds. These results will be compared to the dynamic solutions later.

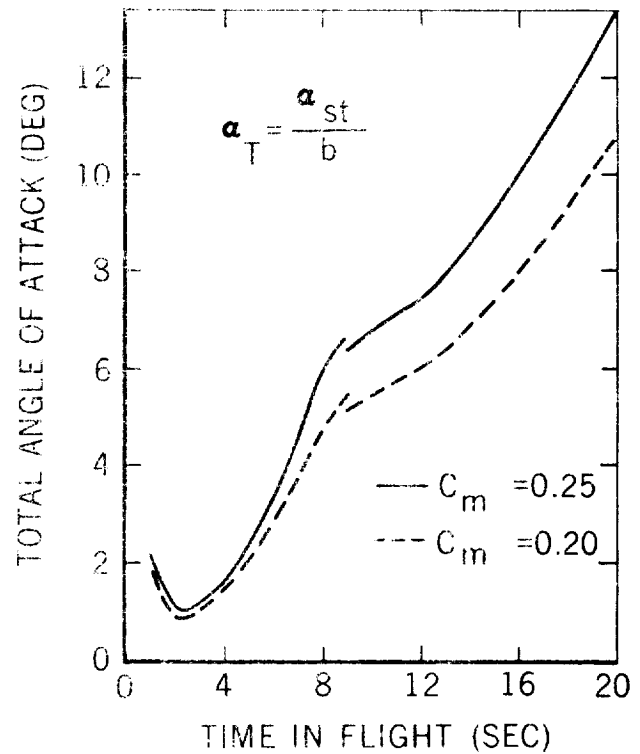


FIGURE 14. TOMAHAWK ROLLING TRIM

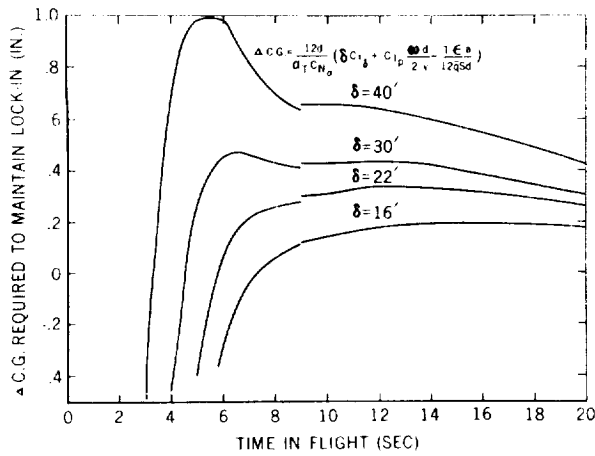


FIGURE 15. REQUIRED CENTER-OF-GRAVITY OFFSET TO MAINTAIN LOCK-IN

Dynamic Solution

The dynamic response of the vehicle will now be considered for the asymmetries listed in Figure 10 and a center-of-gravity offset of 0.15 inch in the worst-case orientation. The natural undamped pitch frequency and the roll-rate obtained from the dynamic solution are presented in Figure 16 for the range of fin cants under consideration. The figure shows that for the fin cants considered, the rocket roll rate does return to the undisturbed roll rate after the vehicle breaks out of resonance. The total angle-of-attack-time histories associated with these dynamic roll-rate histories are presented in Figure 17. As indicated by the steady-state solution, the maximum total angle of attack at resonance increases as the time of resonance is delayed, that is, as the fin cant angle is reduced in magnitude.

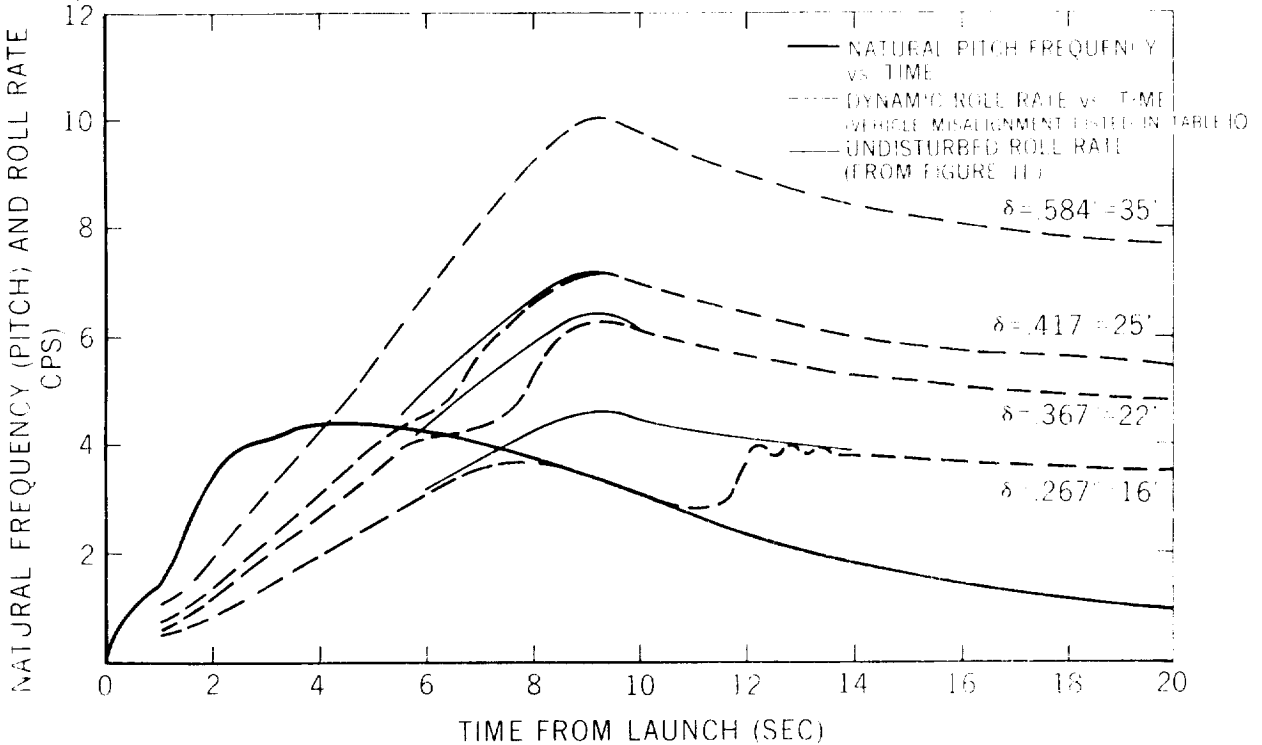


FIGURE 16. DYNAMIC ROLL RATES

A comparison of the dynamic and steady-state solution of the vehicle motion at resonance is presented in Figure 18. The conservatism of the steady-state solution decreases with decreasing fin cant angle. The steady-state solution "underpredicts" the total angle for a fin cant of 16 minutes. This decrease in the conservatism of the steady-state solution can be explained by a brief examination of Figure 15. The increment between the maximum allowable $\Delta C.G.$ and the actual $\Delta C.G.$ of 0.15 is the driving potential which returns the roll rate to the undisturbed value after breakout occurs. This increment, or driving potential, decreases with decreasing fin cant, which results in a lag in the recovery of the roll rate to the undisturbed roll rate. As a result of this lag, the vehicle remains in proximity to resonance, allowing the rolling trim to build in magnitude to a value higher than predicted by the steady-state solution.

The effects of variations in the aerodynamic pitch damping, C_{m_q} , have been evaluated and the results are presented in Figure 19. The rolling trim was calculated with the full value of aerodynamic pitch damping and with one-half the value of aerodynamic pitch damping for two fin cant angles, 16 and 35 minutes. As shown in Figure 19, the effect of varying C_{m_q} is more severe for the lower fin cant, where the maximum total angle increased 30 percent. This increase was only 15 percent for the 35-minute fin cant. Partly because of the reduction in amplitude half-life, the space coning angle for the 16-minute fin cant was also increased. For the 35-minute fin cant angle, C_{m_q} variations have no effect on the space coning angle since the amplitude half-life is virtually unaffected.

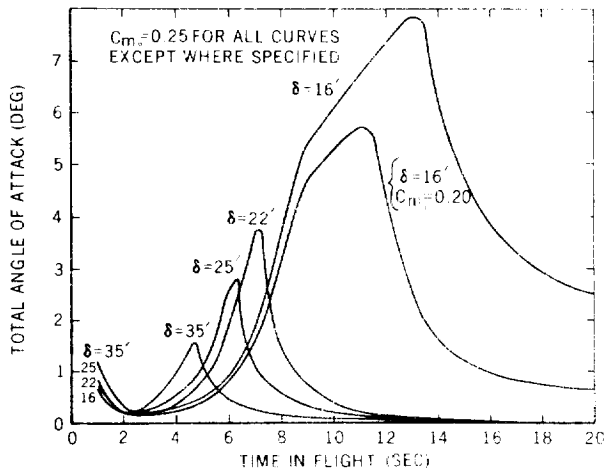


FIGURE 17. DYNAMIC ROLLING TRIM

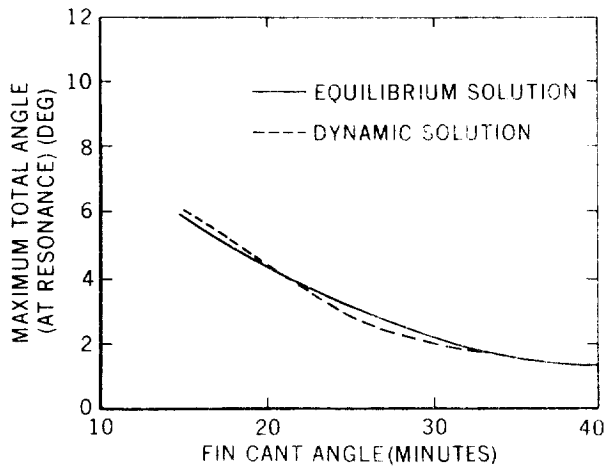


FIGURE 18. COMPARISON OF THE STEADY STATE AND DYNAMIC SOLUTIONS

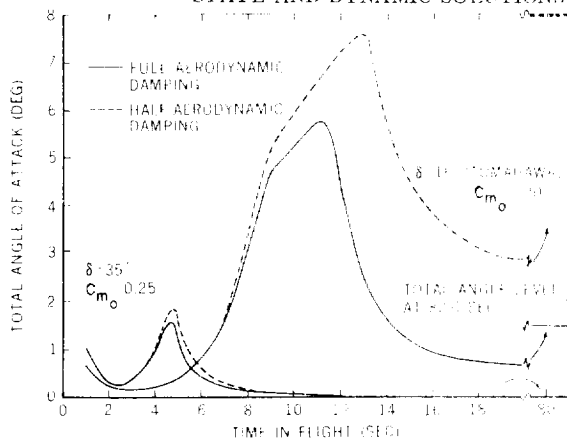


FIGURE 19. EFFECT OF AERODYNAMIC PITCH DAMPING ON THE ROLLING TRIM

Space Coning Motion

A spin-stabilized sounding rocket, upon leaving the atmosphere, behaves as a torque-free gyro, spinning about its center of mass. A unique coning angle and precession rate exists for each set of vacuum pitch, yaw, and roll rates. These vacuum angular rates result from the post resonance residual motions.

The equilibrium space coning angle (15) is calculated as

$$\tan \frac{1}{2} \theta = \frac{1 \sqrt{q^2 + r^2}}{I_{xx} p R_0} \quad \left| \quad t = t_v \right.$$

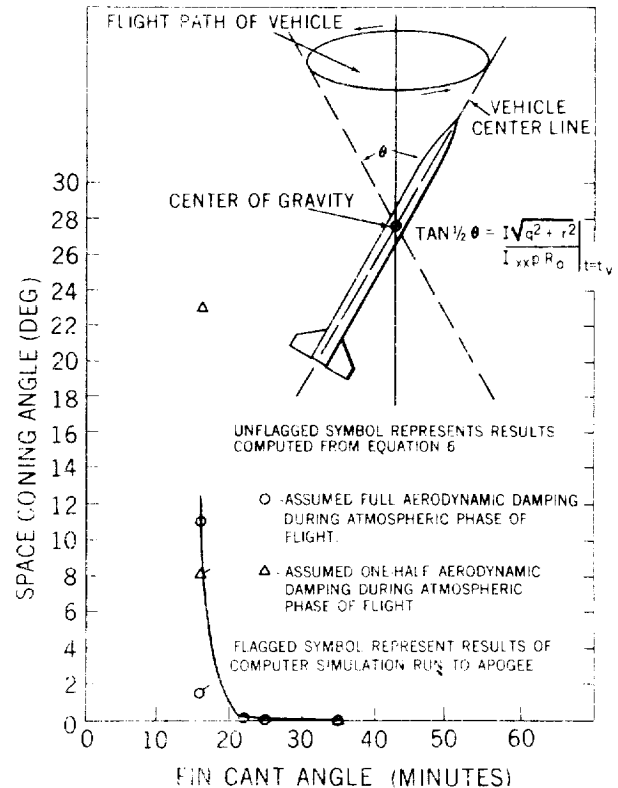


FIGURE 20. SPACE CONING MOTION

The space coning angle computed for the range of roll rates investigated in this study along with the axis system is presented in Figure 20. The above solution is for the equilibrium condition with no reference to the time required to reach the equilibrium condition. However if a vehicle configuration can be found for which the equilibrium body orientation is within the vehicle orientation restrictions, the time required to reach equilibrium conditions becomes academic.

Fin Cant Selection

For a single-stage, high-performance vehicle such as Tomahawk, the choice of fin-cant angles, and therefore the time of resonance, is very important. For structural reasons it is desirable to have pitch-roll resonance with its accompanying rolling-trim angle of attack at a time other than maximum dynamic pressure. The maximum dynamic pressure of the Tomahawk vehicle approaches 20,000 psi at 8.0 seconds in flight. The intermediate fin cant angles can be eliminated since the vehicle would be in resonance in the region of maximum dynamic pressure. The large angles of attack at resonance and the resultant large

space coning motion due to the decrease in damping after thrust termination prohibit the use of the low fin cant angles. The only remaining time in the flight for resonance to occur is early in the flight before the buildup of the dynamic pressure and vehicle temperatures due to aerodynamic heating. The vehicle motion restraints included in the vehicle requirements stipulate a maximum roll rate of 10 cps. This places an upper limit on the fin cant angle of 35 minutes. This fin setting is acceptable from all aspects analyzed and is recommended as the operational fin cant setting for the single-stage Tomahawk vehicle.

Conclusions

1. The Tomahawk vehicle has the impulse to lift the required payload to the required altitude. In addition, the payload weight range can be extended to heavier payloads by interchanging the standard nose cone (3:1 ogive) with lower drag configurations.

2. The present second-stage fins produce adequate stability to fly payloads as light as 65 pounds with the 3:1 ogive nose. The minimum flyable weight is slightly higher for the low-drag configurations; however, they are only used for heavier payloads.

3. The optimum fin cant setting is 35 minutes. This fin cant produces a peak roll-rate of 10 cps and a vacuum roll-rate of 6.5 cps. The vehicle can be flown at lower peak roll rates—as low as 6.5 cps if it is determined that the vehicle can structurally withstand the resulting higher angles at the maximum loading condition. Otherwise, the tolerances on the misalignments and offsets will have to be reduced in order to allow reduction of the peak roll rate.

List of Symbols

A_1 Constant (dimensionless)

a Point of thrust application measured from center-of-gravity, inch

b Reciprocal of magnification factor (dimensionless)

C Fin center of pressure measured from the base, feet

C_D Drag coefficient at zero angle of attack (dimensionless)

C_{lp} Roll damping coefficient $\frac{\partial C_l}{\partial \left(\frac{pd}{2V}\right)}$, per radian

C_l Roll forcing coefficient, per radian

$C_{L\alpha}$ Lift curve slope, per radian

C_{m_0} Moment coefficient at zero angle of attack (dimensionless)

C_{m_q} Pitch damping coefficient $\frac{\partial C_m}{\partial \left(\frac{qd}{V}\right)}$, per radian

$C_{m\alpha}$ Moment coefficient slope at zero angle of attack, per radian

$C_{N\alpha}$ Normal force curve slope, per radian

$C_{n_{p\alpha}}$ Magnus moment (assumed zero)

d Reference diameter, feet

$\Delta C.G.$ Center-of-gravity offset measured from center line, inch

I Pitch moment of inertia, slug-ft²

I_{xx} Roll moment of inertia, slug-ft²

I_{sp} Specific impulse, seconds

L Total vehicle length, feet

m Mass, slugs

p Vehicle roll rate, radians per second

q Pitch rate, degrees per second

\bar{q} Free stream dynamic pressure, lbs/ft²

r Yaw rate, degrees per second

R_0 Conversion factor, from radians to degrees

r_e Distance from nozzle exit plane to center-of-gravity, feet

r_o $\left[r_e^2 - \left(\frac{I}{m} \right) \right]^{\frac{1}{2}}$ by definition, feet

S Reference length, ft²

T Thrust, pounds

t Time, seconds

V Free stream velocity, feet per second

$X_{c.p.}$ Total vehicle center of pressure measured from base, feet

$\overline{X_{c.p.}}$ Nose and afterbody (minus fins) center of pressure measured from the nose, feet

α Angle of attack, degrees

α_T Total angle of attack, degrees

α_{st} Static trim angle of attack, degrees

ϵ	Thrust eccentricity, degrees
θ	Space coning total angle, degrees
ν	Ratio of roll-pitch inertia, (dimensionless)
ω	Natural pitch frequency, radians per second
δ	Fin cant angle, degrees or radians

Identification Symbols:

(F + I)	Fin plus interference
(N + A)	Nose plus afterbody (minus)
(T)	Total Vehicle

Subscripts:

SS	Steady state conditions
V	Vacuum conditions

References

1. "Thiokol Flight Test Proposal TAM 4-66" (February 1966).
2. Stone, G. W.; Connell, G. M.: "Range Safety for the Nike Tomahawk Rocket System with a Nine-Inch Diameter Payload," Sandia Corporation (April 1964).
3. Mayo, E.: "Nike Tomahawk Preliminary Performance Studies," GSFC Document X-721-66-77 (February 1966).
4. Stoney, E., Jr.: "Collection of Zero-Lift Drag on Bodies of Revolution from Free-Flight Investigations," NASA Technical Report R-100 (1961).
5. Hoerner, F.: Aerodynamic Drag, published by the author (1951).
6. Givin, H.; Spring, D.: Stability Characteristics of a Family of Tangent Ogive-Cylinder Bodies at Mach Numbers from 0.20 to 1.5, Army Ballistic Missile Agency, Report No. RG-TR-61-1 (15 June 1961).
7. Morris, N.: A Summary of the Supersonic Pressure Drag of Bodies of Revolution (July 1961).
8. Syvertson, C. A.; Dennis, D. H.: A Second-Order Shock Expansion Method Applicable to Bodies of Revolution Near Zero Lift, NASA Report 1328.
9. Mayo, E. E.; Weisskopf, G. A.; Hutton, C. I., Jr.: Nike Tomahawk Nose Optimization Studies, GSFC Document X-721-65-473 (November 1965).
10. Thiokol Flight Test Proposal TAM-26-66 (June 1966).
11. Survey and Evaluation of a 500 Kilometer, New Sounding Rocket, Booz-Allen Applied Research Inc., BAARINC Report No. 862-3-36-2, prepared under contract no. NAS 5-3752 (November 1965).
12. Muraca, R. J.: An Empirical Method for Determining Static Distributed Aerodynamic Loads on Axisymmetric Multistage Launch Vehicles, NASA Technical Note TN D-3283 (March 1966).
13. Price, D. A., Jr.: Final Report for the Aero-bee 350 Roll Lock-in Study, Contract No. NAS 5-9061, Lockheed Missiles and Space Company, Palo Alto, California.
14. McNeal, D. R.: Description and Users Manual for Roll-Pitch Motion Digital Computer Program, LMSC Report No. M-60-64-2, Lockheed Missiles and Space Company, Sunnyvale, California.
15. Gardner, R. E.: Preliminary Range Safety Analysis on the Single Stage Tomahawk, Sandia Corporation (January 1965).
16. Bickford, J. H.: Space Mechanics: Rigid Body Rotation. Electromechanical Design September 1966).